Journal of Alloys and Compounds 509 (2011) 6015–6020

Contents lists available at ScienceDirect

Journal of Alloys and Compounds

journal homepage: www.elsevier.com/locate/jallcom

Effect of ionic liquid amount ($C_8H_{15}BrN_2$) on the morphology of Bi_2Te_3 nanoplates synthesized via a microwave-assisted heating approach

Guangbin Ji, Yi Shi*, Lijia Pan, Youdou Zheng

Jiangsu Provincial Key Laboratory of Photonic and Electronic Materials Sciences and Technology, College of Electronic Science and Engineering, Nanjing University, Nanjing 210093, PR China

ARTICLE INFO

Article history:
Received 29 September 2010
Received in revised form 22 January 2011
Accepted 24 February 2011
Available online 3 March 2011

Keywords:
Bi_2Te_3
Room temperature ionic liquid (RTIL)
1-Butyl-3-methylimidazolium bromide
Microwave heating

ABSTRACT

Bi_2Te_3 crystals with plate-like morphology have been successfully synthesized via a microwave-assisted heating approach in room temperature ionic liquid (RTIL) of 1-butyl-3-methylimidazolium bromide ($C_8H_{15}BrN_2$). Scanning electronic microscopy (SEM) observation of as-synthesized Bi_2Te_3 confirmed their morphology of the hexagonal plates. It was observed that the edge and thickness values of as-synthesized Bi_2Te_3 were in the size of 0.5–2 μm and less than 100 nm, respectively. High-resolution transmission electronic microscopy (HR-TEM) and selected area electron diffraction (SAED) results revealed that the Bi_2Te_3 plates are of single-crystal in nature with the growth direction of $\langle 1\,1\,\bar{2}\,0\rangle$. In addition, as increasing the amount of ionic liquid, SEM results showed a novel evolution process of Bi_2Te_3 morphologies from mixture of Bi_2Te_3 nanorods and nanoplates to regular hexagonal plates, and then nanoplates with many small flecks. Furthermore, a possible mechanism regarding the formation of Bi_2Te_3 plates was proposed as well on the basis of the experimental results. The power factor of Bi_2Te_3 nanoplates is examined to evaluate its thermoelectric property.

1. Introduction

Bi_2Te_3 and its alloys, which possess the high thermoelectric figure of merit (ZT) of 1 near room temperature, are used commercially in low-power cooling and thermoelectric power generators, such as beverage coolers, laser diode coolers, and power generators in space missions [1]. A value of $ZT \sim 3$ is theoretically necessary for thermoelectric devices to compete with traditional refrigeration or air-conditions. Many efforts have been contributed on improving the ZT value of bulk Bi_2Te_3 materials in the past decades [2,3]. Both theoretical predictions and experimental exploration suggest that large improvements in ZT could be achieved in nanostructured systems due to the presence of strong quantum confinement and thermal conductivity reduction effects [4]. Therefore, the synthesis of nanostructural bismuth telluride and its alloys has been the focus of the recent research. Various morphologies of nanostructural bismuth telluride such as nanoparticle [5], nanowire [6], nanofilm [7], nanosheet [8], nanocapsule [9], and nanotube [10] have been prepared till now.

Many synthetic approaches have been selected to prepare Bi_2Te_3 with different nanostructures, suck like ball milling [11], reverse micelle [12], chemical deposition [13], template [14], solvothermal [15], and so forth. For these methods, however, long time, high temperature, high pressure or complicated set up for preparation were normally required, which was difficult to achieve large-scaled productions. Compared to the conventional methods mentioned above, microwave irradiation, as a heating method widely applied in the synthesis of nanomaterials, is becoming a fast growing research area owing to its advantages such as rapid volumetric heating, higher reaction rate, selectivity, and shorter reaction time [16].

Microwaves produced by magnetrons are electromagnetic waves containing electric and magnetic field components. It can be absorbed by materials directly that makes the electromagnetic energy convert to thermal energy. Heat generated from inside of materials accelerates reaction rate, reduces reaction time and energy cost, and makes new material synthesis possible, which conventional heating methods cannot achieve [17]. On the other hand, room temperature ionic liquid (RTIL) is a kind of polar molecules which can absorb microwaves strongly thus lead to a higher reaction rate and shorter reaction time [18]. Meanwhile, RTIL can also be used as surfactants which dramatically affect the process of crystal growth.

To date, studies regarding the preparation of Bi_2Te_3 nanomaterials by microwave heating method are not extensively reported. Previously, Zhu et al. [19] prepared Bi_2Te_3 nanorods and nanoflakes by a microwave-assisted polyol method using Te and $Bi(NO_3)_3$. Jiang et al. [20] and Yao et al. [21] once synthesized Bi_2Te_3 hollow nanospheres and nanosheets/nanotubes by a microwave (-assisted) method, respectively.

* Corresponding author. Tel.: +86 25 86621120; fax: +86 25 86621120.
E-mail address: yshi@nju.edu.cn (Y. Shi).

0925-8388/$ – see front matter © 2011 Published by Elsevier B.V.
doi:10.1016/j.jallcom.2011.02.142

Herein, we report a microwave-assisted method for preparing Bi_2Te_3 plates with homogeneous hexagonal morphology in RTIL of 1-butyl-3-methylimidazolium bromide ($C_8H_{15}BrN_2$). In addition, the important effect of the ionic liquid amount on the morphology evolution of the Bi_2Te_3 particles, and a possible formation mechanism of the Bi_2Te_3 nanostructure were investigated and discussed as well.

2. Experimental

All reagents were commercially available and used without further purification. In a typical procedure, bismuth nitrate ($Bi(NO_3)_3{\cdot}5H_2O$, 0.5 mmol), telluride powder (Te, 0.75 mmol), potassium hydroxide (KOH, 0.3 g) and an ionic liquid 1-butyl-3-methylimidazolium bromide ($C_8H_{15}BrN_2$, 1 g) were dissolved in 15 mL of ethylene glycol. After vigorous magnetic stirring for 2 h, the solution was put into the microwave oven and heated for 10 min. Microwave assisted reactions were conducted in an 800 W microwave oven, with a 2.45 GHz working frequency. In all experiments, the microwave oven was cycled as follows: on for 40 s, off for 60 s. At the end of the reaction, a great amount of black precipitate was obtained. After cooling to room temperature, the precipitates were centrifuged, washed with water and absolute ethanol in sequence, and dried under vacuum at 60 °C for 12 h. The phase structure characterization of the samples was examined by X-ray diffraction (XRD) in the 2θ range 20–80° using Cu-Kα X-ray source ($\lambda = 0.15418$ nm) with voltage and current of 40 kV and 100 mA, respectively. The morphology of as-prepared samples was observed by a field emission scanning electron microscope (FE-SEM, JEOL S4800) and transmission electron microscope (TEM, JEOL JEM 2100).

3. Results and discussion

The XRD pattern of the as-prepared powders is shown in Fig. 1. All the diffraction peaks can be indexed to a pure rhombohedral phase (space group: $R\bar{3}m$ (166)) of Bi_2Te_3 with lattice constants $a = 0.438733$ nm and $c = 3.04728$ nm (JCPDS no: 15-0863). The XRD pattern indicates that Bi_2Te_3 products with high purity can be obtained.

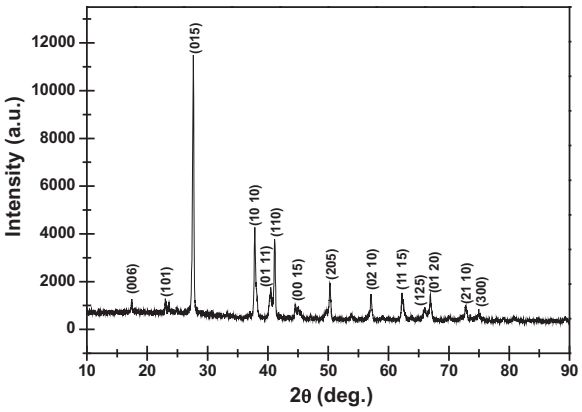

Fig. 1. The XRD pattern of as-synthesized Bi_2Te_3 plates.

Fig. 2 shows the FESEM images of the as-prepared samples in different magnifications. It was found that these hexagonal platelet-like Bi_2Te_3 crystals possess a edge in the length of ~0.5–2 μm, and the thickness less than ~100 nm. The chemical composition of these plates is further determined by energy dis-

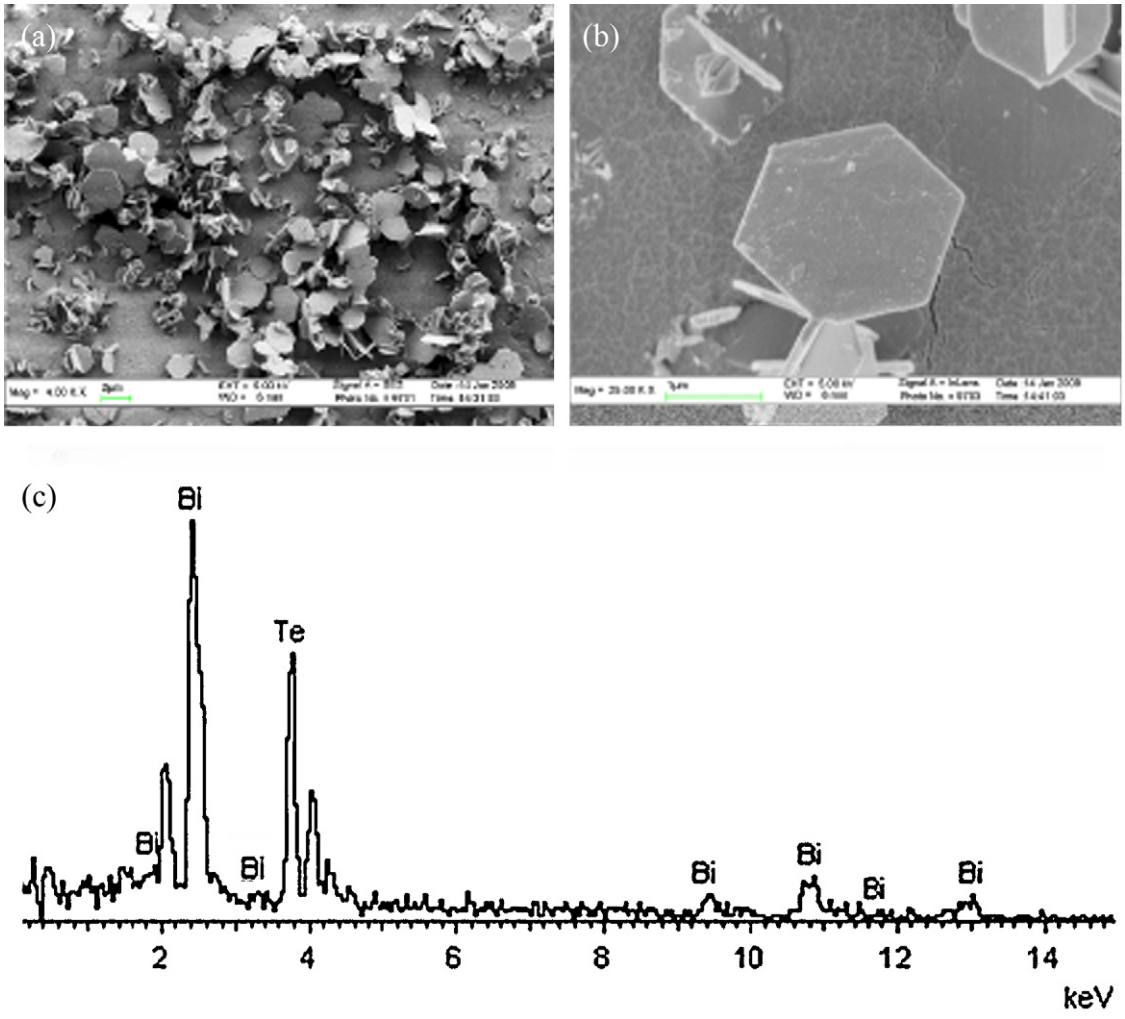

Fig. 2. Representative SEM images (a, b) with different magnifications and EDS spectrum (c) of as-synthesized Bi_2Te_3 plates.

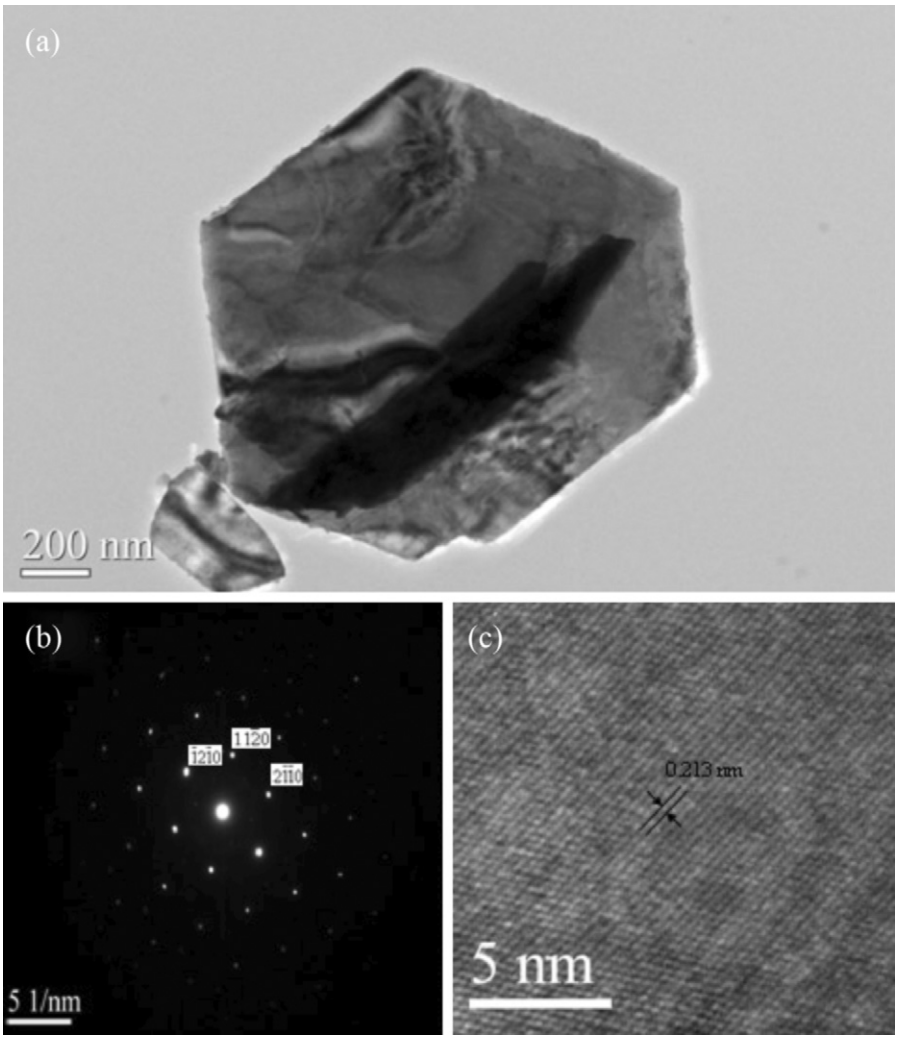

Fig. 3. Representative TEM image of Bi_2Te_3 plates (a), SAED pattern (b) and HR-TEM image of single Bi_2Te_3 plate.

persive X-ray spectroscopy (EDS) (see Fig. 2c). Quantification of the relevant EDS peaks gave an atomic ratio of 0.4107:0.5893 for Bi:Te, which is consistent with the expected value.

As demonstrated in Fig. 3(a), TEM image shows the morphology of hexagonal Bi_2Te_3 plates. The ripple-like patterns are due to the strain resulting from the bend of super-thin nanoplates [22]. The corresponding SAED pattern (Fig. 3b) can be identified as the [0 0 0 1] zone axis projection of the hexagonal Bi_2Te_3 reciprocal lattice. The top–bottom surfaces are {0 0 0 1} facets, whereas the six side surfaces are $\{1\,1\,\bar{2}\,0\}$ facets. The diffraction observation indicates that $\langle 11\bar{2}0\rangle$ is the growth directions for developing the hexagonal crystals. The as-prepared Bi_2Te_3 nanoplates are single crystal and dominated by {0 0 0 1} facets. Corresponding high resolution TEM images (shown in Fig. 3c) of selected areas of Bi_2Te_3 nanoplatelets confirm that the nanoplates are single crystal and defect-free, which <0 0 0 1> is the slowest growth direction [23].

The main reason may be due to their anisotropic structure, though the growth mechanism for the formation of the hexagonal Bi_2Te_3 nanoplates is still unclear. Bi_2Te_3 owns an intrinsic anisotropic layered crystal structure. A period of Bi_2Te_3 crystal has 15 layers stacked along the *c*-axis and presents the combination of three hexagonal layer stacks of composition in which each set consists of five atoms (Te1–Bi–Te2–Bi–Te1). Between two adjacent Te1 layers, there are van der Waals bonds, while all others, covalent bonds [15]. This special bonding structure dominates the shape of the primary Bi_2Te_3 particles and leads to the faster growth of crystal along the top–bottom crystalline plane compared with that along the *c*-axis as the crystalline facets tend to develop on the low-index planes to minimize the surface energy when growing [23]. In the process of the synthesis, it could be found that ionic liquid played an important role in the formation of the nanoplates. The Bi_2Te_3 nanocrystals prepared without adding ionic liquid are mainly composed of irregular shapes with the wide size distribution. It was likely that the ionic liquid acted as a capping reagent or a surfactant. The added ionic liquid capped on the surfaces of Bi_2Te_3 nanocrystals might further enlarge the energetic difference between the top and bottom facets and the side facets, resulting in the anisotropic growth [24].

Fig. 4 shows the morphology of Bi_2Te_3 nanostructure prepared with 0.6 g ionic liquid $C_8H_{15}BrN_2$. It can be seen that the majority are Bi_2Te_3 nanoplates (Fig. 4b) and the others are Bi_2Te_3 nanorods (Fig. 4c). The Bi_2Te_3 nanorods may be induced from its interior lattice structure and the absence of surfactant protection, which has a trend to obtain the wire-like structures. This phenomenon was similar with that of Zhao et al. [25].

Fig. 5 shows the FE-SEM images of the samples prepared with different amount of $C_8H_{15}BrN_2$. Fig. 5(a) shows the SEM image of the Bi_2Te_3 nanoplates prepared with 0.6 g $C_8H_{15}BrN_2$. Both Bi_2Te_3 nanoplates and nanorods can be formed. Fig. 5(b) shows the SEM image of the Bi_2Te_3 nanoplates prepared with 0.8 g $C_8H_{15}BrN_2$, it can be seen the regular Bi_2Te_3 hexagonal nanoplates. The morphology of Bi_2Te_3 in Fig. 5(b) is similar with that in Fig. 2(b). It is initially

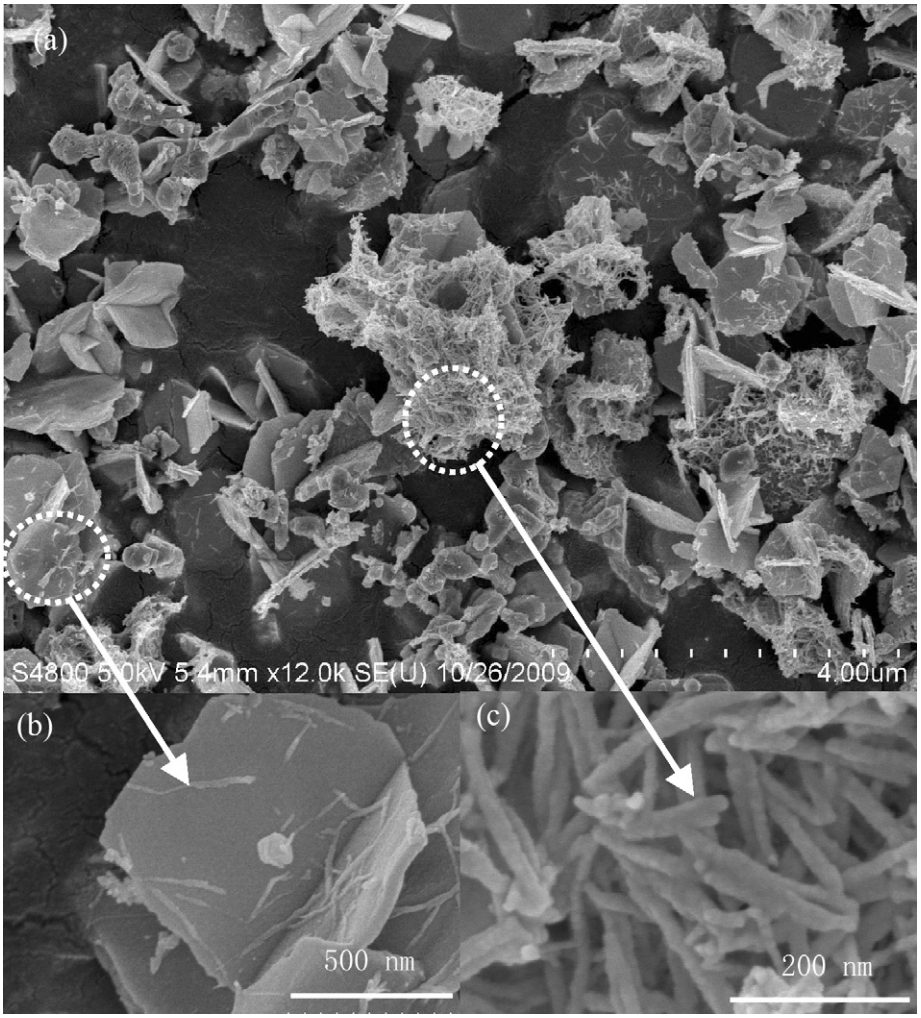

Fig. 4. Typical SEM images of Bi_2Te_3 nanoplates synthesized with 0.6 g $C_8H_{15}BrN_2$.

concluded that the 1 g $C_8H_{15}BrN_2$ is the appropriate amount of ionic liquid which Bi_2Te_3 nanoplates with high purity can be obtained. With increasing of the induced amount of ionic liquid, the morphologies of Bi_2Te_3 nanoparticles change. Several new interesting morphologies of Bi_2Te_3 hexagonal nanoplates with many small flecks (Fig. 5c and d) can be observed.

It can be concluded from the above results that different amount of ionic liquid plays an important role in the morphology control of Bi_2Te_3 nanostructures. A possible mechanism for the formation of Bi_2Te_3 nanostructures with ionic liquid was proposed. As we known, as new types of environmentally friendly reaction media, ionic liquids have many unique properties such as extremely low volatility, wide temperature range in liquid state, good dissolving ability, high thermal stability, excellent microwave absorbing ability, high ionic conductivity, wide electrochemical window, and non-flammability, etc. [18,26]. The ionic liquid $C_8H_{15}BrN_2$ consists of cation $[C_8H_{15}N_2]^+$ and anion Br^-. The high ionic conductivity and polarizability of $[C_8H_{15}N_2]^+$ make it an excellent microwave-absorbing agent, thus leading to a high heating rate and a significantly shortened reaction time.

Considering the special lattice structure of Bi_2Te_3, the ionic liquid holds the layered-like rhombohedral structure. The hexagonal cell is formed by a set of layers perpendicular to the third-order axis of symmetry (*c*-axis). In this complex structure, interlayer cleavage might appear easily along the *c*-axis, and the uniform morphologies were hard to be synthesized [27].

Previously, it is widely believed that the ionic liquid could prevent the aggregation of Bi_2Te_3 nucleus. In addition, because of the possible controlling caused by their different adsorption energies on various basal planes of such rhombohedral structure, $C_8H_{15}BrN_2$ molecules might be able to modulate the growth kinetics of the Bi_2Te_3 seeds thus modify the physical–chemical characteristics of the surface [28]. The $C_8H_{15}BrN_2$ molecules might be adsorbed on these crystal planes due to layer-like structure and weak interfacial interaction (such like van der Waals force) along *c*-axis, which could possibly decrease the growth rate along *c*-axis significantly. Therefore, it is reasonable to deduce that Bi_2Te_3 of hexagonal plates can be obtained under condition of an optimal amount of $C_8H_{15}BrN_2$ (1.0 g was considered as an optimal amount in this present study). Namely, if the employed amount of $C_8H_{15}BrN_2$ (amount of 0.6 g was selected in the present study) was lower than the optimal value, Bi_2Te_3 nanorods while others nanoplates would be formed as parts of Bi_2Te_3 nucleus will not be affected by the $C_8H_{15}BrN_2$ and will grow along *c*-axis in a certain extent. On the contrary, Bi_2Te_3 nucleus could grow on the formed nanoplates with small flecks (as displayed in Fig. 5d) when the used amount of $C_8H_{15}BrN_2$ was higher than the optimal one (amount of 1.8 g was selected in the present study), because of the weak surface tension of the ionic liquid which could amalgamate with many other inorganic matters and raise their nucleation rates [29]. The detailed formation mechanism of these Bi_2Te_3 plates with small flecks in ionic liquid under microwave heating needs to be further investigated.

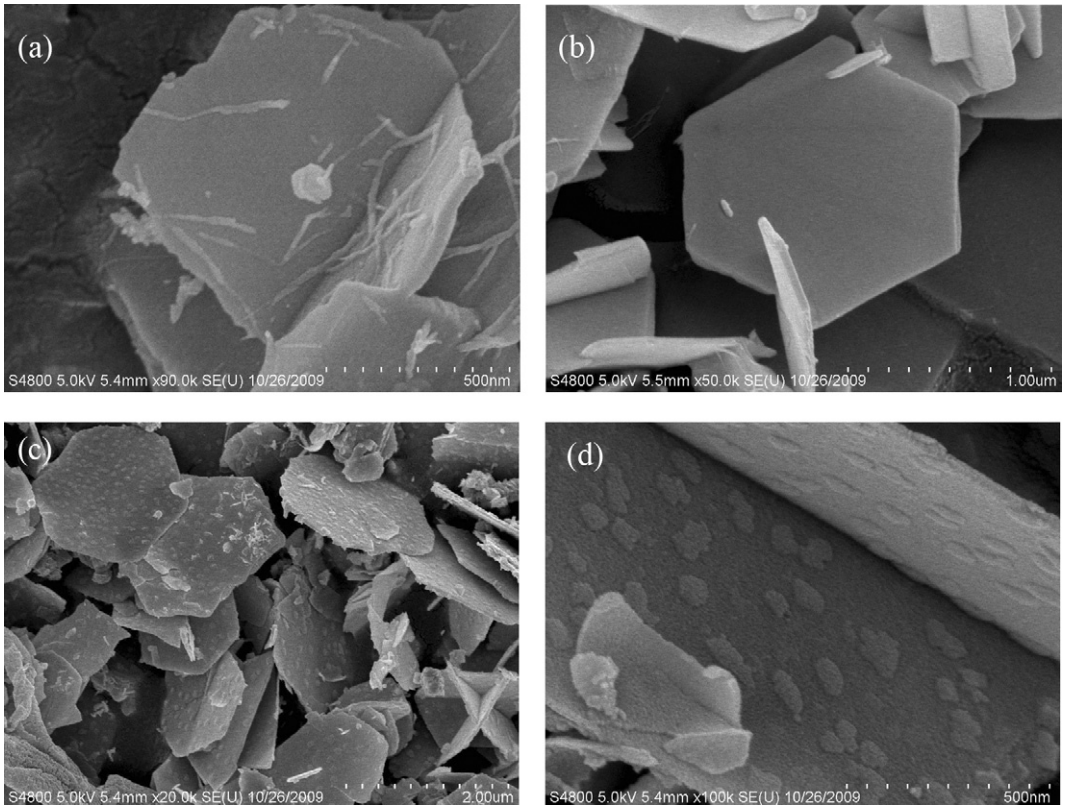

Fig. 5. Typical SEM images of Bi_2Te_3 obtained at different $C_8H_{15}BrN_2$ conditions: 0.6 g (a), 0.8 g (b), 1.0 g (c), 1.8 g (d).

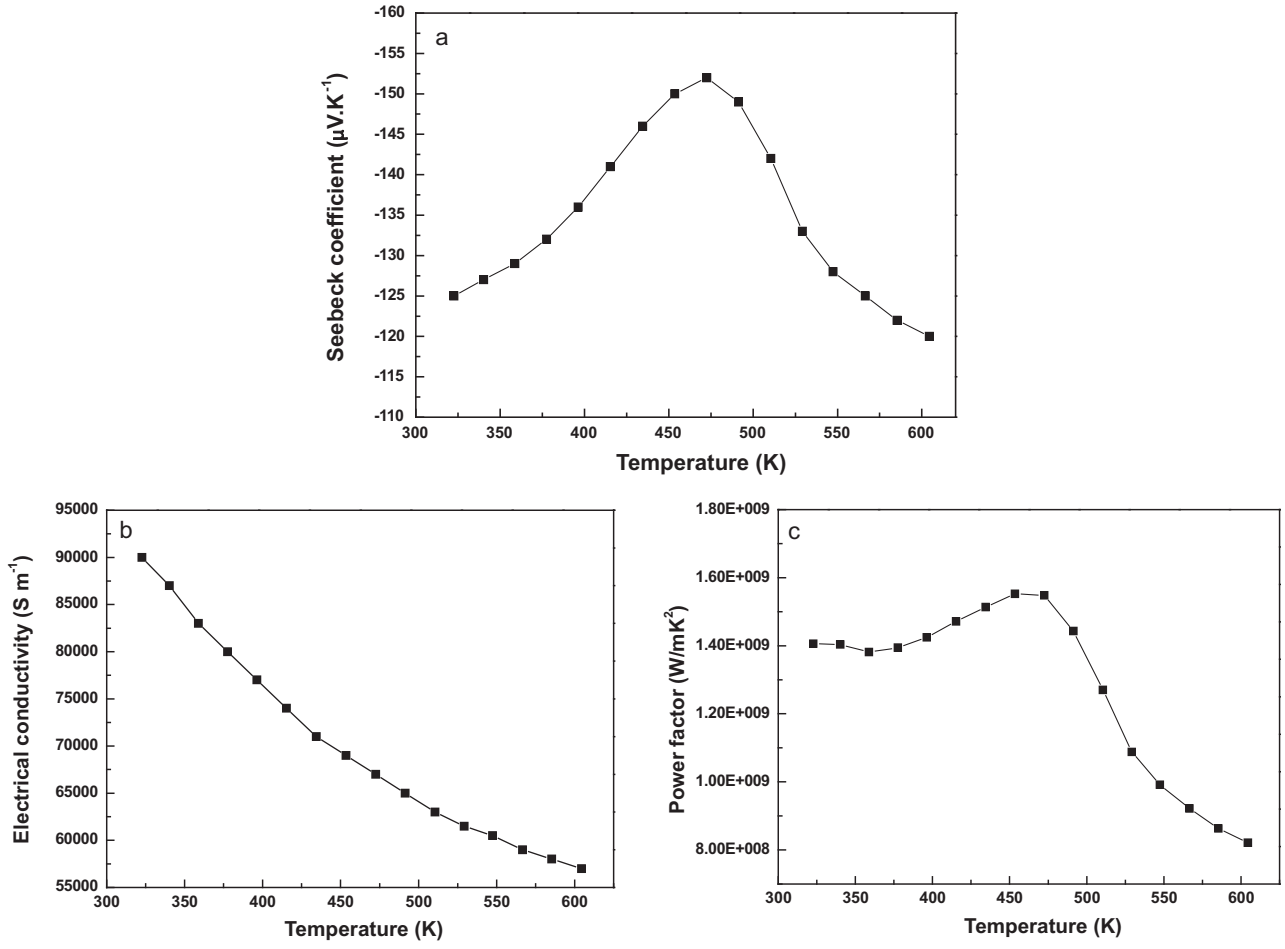

Fig. 6. Seebeck coefficient (a), electrical conductivity (b) and power factor (c) dependence on temperature of Bi_2Te_3 nanoplate synthesized with 1.0 g $C_8H_{15}BrN_2$ via a microwave-assisted heating method.

Fig. 6 shows the curve of Seebeck coefficient, electrical conductivity, and power factor dependence on temperature of Bi_2Te_3 nanoplates synthesized with 1.0 g $C_8H_{15}BrN_2$ via a microwave-assisted heating method. From Fig. 6(a), it can be seen that the Seebeck coefficient of Bi_2Te_3 is negative which indicates that the Bi_2Te_3 synthesized is n-type semiconductor. The Seebeck coefficient increases as the temperature in a low temperature range and get a maximum of 152 uV/K at 473 K. In Fig. 6(b), it can be seen that the electrical conductivity of Bi_2Te_3 decreasing as the temperature increasing. The Seebeck coefficient and electrical conductivity are similar with and higher than the results presented in recent research previously [15]. As show in Fig. 6(c), the power factor of Bi_2Te_3 nanoplates gets a maximum at about 450 K. It has been enhanced to some extent but not significantly. As we know, numerous boundaries or interfaces in nanomaterials will make phonons highly scattered and reduce the thermal conductivity efficiently which can improve ZT significantly. The thermal conductivity and ZT needs to be characterized and further investigated.

4. Conclusions

In this study, Bi_2Te_3 plate-like crystals with homogeneous hexagonal morphology have been successfully synthesized by the microwave-assisted heating in the ionic liquid $C_8H_{15}BrN$. The present results show that $C_8H_{15}BrN_2$ plays an important role in the formation of Bi_2Te_3 crystals with different morphologies. It was observed that both Bi_2Te_3 nanoplates and nanorods were obtained in the presence of 0.6 g $C_8H_{15}BrN_2$, and the morphology of Bi_2Te_3 crystal changes to nanoplates with small flecks on while increasing the amount of $C_8H_{15}BrN_2$.

Acknowledgements

This work is financially supported by China Postdoctoral Science Foundation (20080430164 and 200801366), Jiangsu Postdoctoral Science Foundation (0801040B), National Natural Science Foundation of China (no. 50701024) and National Key Project of Fundamental Research (973, no. 2007CB936300).

References

[1] Y.C. Lan, A.J. Minnich, G. Chen, Z.F. Ren, Adv. Funct. Mater. 19 (2009) 1.
[2] E. Koukharenko, N. Frety, V.G. Shepelevich, J.C. Tedenac, J. Alloys Compd. 299 (2000) 1024.
[3] D.Y. Chung, T. Hogan, P. Brazis, M. Rocci-Lane, C. Kannewurf, M. Bastea, C. Uher, M.G. Kanatzidis, Science 287 (2000) 1024.
[4] M.S. Dresselhaus, G. Chen, M.Y. Tang, R.G. Yang, Adv. Mater. 19 (2007) 1043.
[5] M. Scheele, N. Oeschler, K. Meier, Adv. Funct. Mater. 19 (2009) 3476.
[6] S.W. Jun, K.Y. Lee, T.S. Oh, J. Korean Phys. Soc. 48 (2006) 1708.
[7] R. Rahul, R.K.A. Velu, International Conference on Advanced Computer Theory and Engineering, 2008, p. 817.
[8] Z.L. Sun, S.C. Liufu, Q. Yao, Mater. Chem. Phys. 121 (2010) 138.
[9] T. Sun, T.J. Zhu, X.B. Zhao, Acta Chim. Sinica 63 (2005) 1515.
[10] Z. Wang, F.Q. Wang, H. Chen, L. Zhu, H.J. Yu, X.Y. Jian, J. Alloys Compd. 492 (2010) L50.
[11] B. Poudel, Science 320 (2008) 634.
[12] E.E. Foos, R.M. Stroud, A.D. Berry, Nano Lett. 1 (2001) 693.
[13] M. Toprak, Y. Zhang, M. Muhammed, Mater. Lett. 57 (2003) 3976.
[14] A.L. Prieto, M.S. Sander, M.S. Martin, R. Gronsky, T. Sands, A.M. Stacy, J. Am. Chem. Soc. 123 (2001) 7160.
[15] X.B. Zhao, X.H. Ji, Y.H. Zhang, T.J. Zhu, J.P. Tu, X.B. Zhang, Appl. Phys. Lett. 86 (2005) 062111.
[16] L. Guo, G.B. Ji, X.F. Chang, Nanotechnology 21 (2010) 035606.
[17] Y. Jiang, Y.J. Zhu, G.F. Cheng, Cryst. Growth Des. 6 (2006) 2175.
[18] M. Antonietti, D.B. Kuang, B. Smarsly, Y. Zhou, Angew. Chem. Int. Ed. 43 (2004) 4988.
[19] B. Zhou, Y. Zhao, L. Pu, J.J. Zhu, Mater. Chem. Phys. 96 (2006) 192.
[20] Y. Jiang, Y.J. Zhu, L.D. Chen, Chem. Lett. 36 (2007) 382.
[21] Q. Yao, Y.J. Zhu, L.D. Chen, Z.L. Sun, X.H. Chen, J. Alloys Compd. 481 (2009) 91.
[22] X.Y. Kong, Y. Ding, R. Yang, Z.L. Wang, Science 303 (2004) 1348.
[23] W.G. Lu, Y. Ding, Y.X. Chen, J. Am. Chem. Soc. 127 (2005) 10112.
[24] W.Z. Wang, B. Poudel, J. Yang, D.Z. Wang, Z.F. Ren, J. Am. Chem. Soc. 127 (2005) 13792.
[25] T. Sun, X.B. Zhao, T.J. Zhu, J.P. Tu, Mater. Lett. 60 (2006) 2534.
[26] Y.J. Zhu, W.W. Wang, R.J. Qi, X.L. Hu, Angew. Chem. Int. Ed. 43 (2004) 1410.
[27] D.M. Rowe, CRC Handbook of Thermoelectrics, London: CRC Press, 2006.
[28] Y.G. Sun, Y.N. Xia, Science 298 (2002) 2176.
[29] J.M. Cao, B.Q. Fang, J. Wang, Prog. Chem. 17 (2005) 1028.